

Prenatal and Postnatal Exposure to Cell Phone Radiation and its Possible Impact on the Development of Albino Rat Testicular Tissue Light and Electron Microscopic Study

Original
Article

Abdelmonem Awad Hegazy, Marwa M. Ahmad, Noha Ali Abd Almotaleb and Joseph Amin Aziz

Department of Anatomy, Faculty of Medicine, Zagazig University, Zagazig, Egypt

ABSTRACT

Introduction: Perinatal periods are critical phases in the development of testis, and it is sentient to the surrounding environmental pollutants. Electromagnetic radiation (EMR) exposure as a consequence of excessive use of cell phones might be one of such pollutants.

Aim of the Work: This study was designed to evaluate the impact of pre-and postnatal exposure to cell phone radiations on the development of rats' testes.

Material and Methods: Sixteen healthy pregnant female rats were used in the current work. The dams were exposed to EMR of cell phone 2 hours /day from the 6th day of pregnancy, throughout lactation until weaning. We also used corresponding control dams kept away from any radiation. The male pups of both groups were subdivided into three groups (n = 10); according to their age at the time of scarification; group A; scarified at first postnatal day (PND 1), B (PND 21), and C (PND 70). Testes of each group were excised and processed for light (LM) and electron microscopy (EM) studies. Assessment of oxidative parameters, semen analysis and morphometric analysis were conducted on each group.

Results: Various degenerative changes in the structure of rat testis were noticed in EMR-exposed animals which were assured by the significant changes in morphometric parameters. Besides, the oxidative stress status because of EMR-exposure was evident. Sperm parameters of rats at PND 70 were markedly decreased in the exposed animals compared with controls regarding sperm count and motility with an increase in abnormal forms.

Conclusion: Serious effects might result from excessive EMR exposure on developing testis.

Received: 18 April 2021, **Accepted:** 24 June 2021

Key Words: Anatomy, development, mobile phone, testes.

Corresponding Author: Marwa M. Ahmad, MD, Department of Anatomy, Faculty of Medicine, Zagazig University, Zagazig, Egypt, **Tel.:** +20 10 6650 0159, **E-mail:** marwaahmed515@gmail.com

ISSN: 1110-0559, Vol. 45, No. 3

INTRODUCTION

Our lifestyle has been facilitated by many electronic devices like microwave ovens, wireless networks, and mobile phones. Despite their great importance, they could carry a big challenge to the general health due to possible pollutions induced. This necessitates regular research to investigate any possible change in different body tissues. Mobile phones have been accused of emitting a heavy network of Electro-Magnetic-Radiation (EMR). All human tissues can be penetrated by EMR rendering such radiation as a new pollutant. Serious changes in biological parameters might result from the cumulative effect of EMR^[1]. Placing mobile phones and portable computers in the pockets and on the legs of humans makes the genital region to be highly exposed to EMR^[2].

Exposure to EMR could disturb the redox environment of cells with excess production of reactive oxygen species (ROS) that can affect the reproductive system in both animals and humans^[3]. The induced oxidative stress might affect postnatal development in the form of decreased

weekly body weight gain and delay in some anatomical and physiological developments such as teeth and hair appearance and eye-opening. ROS has adverse effects on physiological reproductive functions like maturation, fertilization, embryo development, and pregnancy. This could be attributed to interference between the impact of oxidative stress and growth factors such as insulin growth factors-I^[4]. It also might explain the increased decline in human fertility reported nowadays^[5].

The International Agency for Research on Cancer (IARC) of the World Health Organization (WHO) is labeling cell phone radiation as "possibly carcinogenic to humans". Such radiation has been added to the list of carcinogenic agents; therefore, pregnant women and children need to reduce their exposure to radiofrequency/microwave emissions as much as possible to avoid possible complications^[6].

Therefore, the current study aimed to elucidate the structural alternations in the testes of offspring in response to maternal and postnatal exposure to cell phone radiation.

MATERIALS AND METHODS

Experimental animals

The present study was conducted on sixteen healthy non-pregnant adult female albino rats weighing 150-250 gm obtained from the Scientific and Medical Research Center (SMRS) at the Faculty of Medicine, Zagazig University. Animals were kept for acclimatization in separate hygienic stainless-steel cages at a controlled temperature ($23\pm 2^\circ\text{C}$) and humidity ($60\pm 5\%$) in a (12:12-h light: dark cycle) artificially illuminated room, completely free from chemical contamination. The animals were fed with the standard laboratory food and allowed free access to it and water. All rats were handled following the standard guide for the care and use of laboratory animals^[7].

Experimental design

Every morning, a Vaginal smear is carried out for each virgin female to determine the estrous cycle. An estrous female was confirmed by the presence of cornified cells in the vaginal smear. Eight males were used for mating with pro-estrous female rats at a ratio of 2:1 respectively in each cage. The zero days (D0) of gestation was determined by the presence of sperm in the vaginal smear. The pregnant rats were then randomly divided into two equal groups, 8 rats each. Group I (control) was kept away from cell phone radiation. Group II (exposed) was exposed to cell phone radiation 2 hours /day starting from the 6th day of gestation and during lactation up to the weaning of the offspring^[8]. After delivery, the sex of pups was determined; the female pups were excluded. Male pups of group I (control) were kept away from radiation, while those of group II (EMR-exposed) continued exposure to radiation until post-natal day 70 (PND 70). So finally, we had two groups of pups (control and EMT exposed); each group contained 30 pups which then subdivided into three subgroups (10 pups each) according to their age at the time of scarification, as follows:

Group I (control animals): IA (n=10): Male pups were sacrificed on 1st PND “newborn animals”.

IB (n=10): Male pups were sacrificed on PND 21 “age of weaning”^[9].

IC (n=10): Male pups were sacrificed on PND 70 “age of puberty”^[10].

Group II (EMR-exposed animals) (n=30; 10 pups each): IIA, IIB, and IIC: were corresponding in sacrifice day to those of the control group.

The animals of group II were exposed routinely to EMR emitted from a cell phone, and the exposure duration was 2 hr/day, 6 days/week^[11]. The used cell phone (Nokia 106- made in Vietnam) was with frequency 900-1800 MHz, pulsed at GSM (global system for mobile) mode; specific absorption rate (SAR) value was 2.0 -1.23 W/kg. The cell phone was put in the middle of the cage top to ensure that there was equal electromagnetic radiation to the whole body of the animals in the cage^[10].

The used cell phone was kept on continuously (auto redial) for 100 min daily and then as calling mode (to another phone number) for 20 min. Animals in group I (control) group were put in a separate place to make sure that it is not exposed to any radiation^[12].

At the end of the experiment, all animals were anesthetized by intraperitoneal injection of ketamine (90 mg/kg body weight)/ xylazine (15mg/kg)^[13]; their abdominal and pelvic cavities were opened; testes and epididymides were dissected out for histological and biochemical studies.

Determination of body and testicular weights

Every rat pup was weighed at the time of scarification using a delicate scale to compare the weights between the two groups. After dissection, the freshly removed (RT testis) from rats were also weighed and the relative testicular weight was calculated as the ratio between the absolute weight of the testis and the body weight. The collected data were statistically analyzed.

Tissue preparation for LM and EM study

Tissue specimens (RT testes) were immediately fixed in 10% neutral buffered formalin for 24 h, washed and dehydrated with conventional ascending grades of alcohol, cleared in xylol, then embedded in paraffin. 5 μm thick paraffin sections were stained with hematoxylin and eosin (H&E) for studying the histopathological structure of the testis. as the ratio of testes (wet weight, mg) to BW (g) as the ratio of testes (wet weight, mg) to BW (g)^[14]. LM (Leica ICC50W) in the Image Analysis Unit of the Department of Anatomy and Embryology was used for slide analysis.

For EM study, 1-2 mm sized testicular specimens were fixed in glutaraldehyde and osmium tetroxide, and then dehydrated. Ultrathin sections were stained by uranyl acetate and lead citrate^[15]. Then, sections were examined with JOEL transmission electron microscopy (TEM) at Al Mansoura University, Cairo, Egypt.

Assessment of oxidative parameters

Left testes specimens were minced and homogenized after being weighed in a Teflon-glass homogenizer with a buffer containing 1.15% KCl to obtain 1:10 (W/V) whole homogenate. The mixture was centrifuged at 3000 r.p.m (+4 $^\circ\text{C}$) for 15 min to determine malondialdehyde (MDA) level and superoxide dismutase (SOD) activity, then homogenates were centrifuged at 5000 r.p.m for 50 min to measure the level of reduced glutathione GSH^[16]. SOD activity was expressed as units/min/mg protein according to method described by McCord and Fridovich^[17] method. GSH reactivity was measured at 405 nm by using a commercial kit (Biodiagnostic, Egypt)^[18]; and the level of MDA was determined as a thiobarbituric acid reactive substance (TBARS)^[19].

Epididymal sperm examination

Firstly, the right epididymis from male pups on PND70 was kept in PBS and incubated at 37 $^\circ\text{C}$ for 60 min for

determination of the sperm count, sperm motility, and abnormal forms.

a Determination of the sperm count

According to the method of Yokoi *et al.*,^[20] the right caudal epididymis was minced by a scissor into 5 ml of physiological saline and were placed in a rocker for 10 min, then incubated for 2 min at room temperature, then a fixative/staining solution (containing 5g sodium bicarbonate, 1 ml of 35 % formalin and 25 mg eosin per 100 ml of distilled water) was used to dilute the resulting fluid at 1:100. Using a hemocytometer, the sperm count was determined. Nearly, each counting chamber had 1 ml of diluted sperm suspension which settled down for 5 min then the sperm count was assessed using a light microscope at 200 × magnification and expressed as x10⁶ sperm/ml.

b Determination of living and dead sperms & sperm motility percentage

The epididymal head was cut in Petri dish to release all sperms and 2 ml normal saline was added. On a slide, two drops of eosin – nigrosine stain were added to one drop of semen mixture to make a thin film on. Percentage of live, dead sperms were measured^[21].

For the sperm motility percentage, a slide is placed into the microscopy stage and warmed up to 37°C and 2 drops of Tris buffer solution (Trishydroxymethyl aminomethane 3.63 g, glucose 0.50 g, citric acid 1.99 g, and distilled water up to 100 ml) were placed on the slide and mixed with one drop epididymal fluid. At a magnification of 400, the percentage of motility was estimated and the average of five successive estimations was used as the final motility (%)^[22].

c Determination of morphologically abnormal sperm forms

On a pre-warmed slide 2 drops of Tris buffer solution were placed, then mixed with one drop of epididymal fluid and two droplets of Indian ink stain for one minute. The slide was left to dry off, then at a magnification of 400 light microscopy four hundred sperm cells were examined on each slide, and the abnormal sperm forms were expressed as the percentage^[23].

Morphometric study

The morphometric data were obtained from ten non-overlapping fields in the H&E-stained slides of each animal using a Leica QWin 500 image analyzer (Leica Ltd, Cambridge, UK), in the Anatomy Department, Faculty of Medicine, Zagazig University. Image analysis and morphometry were performed by Image J (FIJI) software to determine the mean diagonal diameter seminiferous tubule. For each seminiferous tubule two perpendicular measurements from the corners were done to get its mean. In addition, the interstitial space was assessed by measuring three dimensions from its center to the basement membrane of the surrounding tubules. Also, germinal epithelial height was measured from the basement membrane to the lumen. All measurements were set in µm.

Statistical analysis

All collected data were computerized and statistically analyzed using Graph Pad Prism 5.01. Quantitative data were expressed as mean ± SD (Standard deviation). Differences between mean values of experimental groups were tested with an unpaired two-tailed t-test. The results were considered statistically significant when the *P*-value of < 0.05.

RESULTS

Mortality

No deaths had been recorded among offspring.

LM examination

Group I (Control group): Examination of H&E-stained sections at 400x of group IA (1st PND) revealed normal testes architecture of this age; formed of multiple solid seminiferous cords lined mainly with Sertoli and gonocytes with their surrounding tunica albuginea. Small groups of fetal Leydig cells were seen within the intertubular space (Figure 1a). In group IB (21st PND), seminiferous cords have started canalization and noticeable lumen could be detected showed lining with different cell layers; spermatogonia and Sertoli cells along the basement membrane and primary spermatocytes lie near the center (Figure 1b), while on 70th PND, the normal architecture of closely packed seminiferous tubules lined with stratified germinal epithelium was noticed. Sperms appeared as an aggregation of filamentous bundles extended into the luminal side (Figure 1c).

Group II (EMR-exposed group): On PND 1, the examination of H&E-stained sections of rats' testes exposed to EMR, showed widely separated seminiferous tubules, mild congestion, and clustering of Leydig cells (Figure 2a), On PND 21, seminiferous tubules appeared with distorted basal lamina with some exfoliated germ cell. The seminiferous epithelium showed many vacuoles. Homogenous acidophilic material was noticed between the interstitial cells (Figure 2b).

As regard 70th PND, there was disturbance of the normal arrangement and stratification of germinal epithelium. The tubules showed hydropic degeneration and the disappearance of sperms. The deposition of homogenous acidophilic material was demonstrated between the seminiferous tubules (Figure 2c).

EM examination

Group I (control group): Examination of ultrathin sections of group IA (1st PND) revealed seminiferous cords with gonocytes located in the center of the tubule having large spherical nuclei and fine chromatin and its cytoplasm contained numerous mitochondria (Figures 3a,b). Sertoli cells were resting on a thin basement membrane with clear oval euchromatic nuclei with a prominent nucleolus and its cytoplasm contained many mitochondria (Figure 3c). Leydig cells and other undifferentiated mesenchymal cells

were seen near a blood vessel, also flat myoid cells were recognized (Figure 3d).

On PND 21, the seminiferous tubules were lined with spermatogonia, Sertoli cells, and primary spermatocytes. The Sertoli cell had a pyramidal euchromatic nucleus and many mitochondria, the spermatogonia had a euchromatic nucleus in addition to many mitochondria within its cytoplasm, also the primary spermatocyte revealed a euchromatic nucleus with many mitochondria and some lysosomes could be observed (Figure 4a). The primary spermatocytes showed a large spherical nucleus containing and Blood testes barrier was demonstrated, also inter cytoplasmic bridge could be seen (Figure 4b). Spermatogonia had rounded euchromatic nuclei with many mitochondria. Sertoli cells had euchromatic nuclei with prominent nucleolus with many mitochondria. The tight junction blood testes barrier was seen in between the cells (Figure 4c). Leydig cells with their oval euchromatic nucleus were still being observed. Their cytoplasm contained mitochondria of different sizes and shapes (Figure 4d).

The electron microscopic study of the adult control rat testes on PND 70th revealed seminiferous tubules surrounded by a thin basement membrane. The spermatogonia were seen along the basement membrane with a euchromatic nucleus and prominent nucleolus. A blood-testis barrier was demonstrated (Figure 5a). The primary spermatocytes have appeared with a large rounded euchromatic nucleus and the cytoplasm showed free ribosomes (Figure 5b). Sertoli cells had large, indented nuclei with finely granular chromatin, in addition to the intracytoplasmic process of Sertoli extended between the primary spermatocytes (Figure 5c). More mature spermatids showed acrosomal cap appeared well-fitted to one pole of the nucleus with a rounded euchromatic nucleus and numerous peripherally arranged mitochondria were seen (Figure 5d). Cross-section in the tail of normal sperm showed its principle, middle and end pieces. The principal piece is formed of nine doublets of microtubules with two central singlets enclosed by fibrous sheath. The end piece has nine doublets with two central singlets covered by cell membrane only (Figure 5e). The Leydig cell showed a euchromatic nucleus and the cytoplasm contained many mitochondria (Figure 5f).

Group II (EMR-exposed group): Examination of the ultrathin section of testis of a rat on PND 1 revealed gonocytes with the disappearance of its nuclear envelop, karyolysis of chromatin, and multiple vacuoles were seen within the cytoplasm (Figure 6a). Sertoli cells with a completely fragmented nucleus and many vacuoles were seen resting on irregular basement membrane (Figure 6b). Leydig cell appeared with the small, indented nucleus and its cytoplasm showed multiple vacuoles. Fibroblast-like cells or undifferentiated mesenchymal cells (most probably) were noticed (Figure 6c).

On PND 21, the seminiferous tubules were lined with the same cell population lining the control group

of the same age group (spermatogonia, Sertoli cells, and primary spermatocytes) resting on a thick basement membrane and flat myoid cells but with intercellular separation. Moreover, many lysosomes were seen (Figure 7a). The primary spermatocytes showed spherical nucleus with blebbing of nuclear membrane, multiple vacuoles, and many mitochondria within the cytoplasm (Figure 7b). Spermatogonia appeared with a euchromatic nucleus and its cytoplasm showed multiple vacuoles, resting on a thick basement membrane (Figure 7c). Sertoli cell's cytoplasm showed multiple vacuoles and mitochondria, its nucleus lost its membrane with the discontinuity of blood testes barrier (Figure 7d). The Leydig cell had an oval euchromatic nucleus with peripheral heterochromatin, lysosomes, and multiple vacuoles within the cytoplasm (Figure 7e).

Examination of the ultrathin section of testes on PND 70th revealed that spermatogonia appeared with an irregular indented heterochromatic nucleus with wide perinuclear cisterna and multiple vacuoles within the cytoplasm. There is a thickening of the basement membrane (Figure 8a). Sertoli cells appeared with a euchromatic nucleus and prominent nucleolus and their cytoplasm contained multiple vacuoles and mitochondria. Thickened basement membrane was noticed. (Figure 8b). Primary spermatocytes appeared degenerated with condensed nuclear chromatin and loss of nuclear envelop; multiple vacuoles were seen in their cytoplasm (Figure 8c). Abnormal spermatids appeared with an eccentric nucleus; moreover, they had acrosomal caps without peripherally arranged mitochondria (Figure 8d). Transverse sections of the mature spermatozoa (mid, principle, and end pieces of sperms) showed disorganization of the outer dense fibers (ODFs) and the microtubules of the axoneme in addition to loss of the mitochondrial sheath of the midpiece (Figure 8e).

Epididymal spermatozoal examination on PND 70

Normal living sperms with normal head, neck, and tail were noticed with normal head, neck, and tail in the control group (Figure 9a), while examination of semen of EMR-exposed group showed some abnormal forms such as sperms with abnormal tail and broken head (Figure 9b) sperms with detached heads (Figure 9c) and others showed short tail (Figure 9d).

Body and testis weights

The body weight was significantly lower in EMR-exposed animals in PND1 and PND 70 groups when compared to the control ones. On the other hand, although both absolute and relative testicular weights declined significantly in EMR-exposed rats on PND 70, the change was insignificant between the control and exposed pups on PND 1 and PND 21 (Table 1, Figure 10).

Determination of oxidative parameters

MDA values recorded a significant increase among all EMR-exposed animals when compared to the control

ones (Figure 11), while SOD levels showed a significant decrease in EMR-exposed groups (Figure 12). Regarding GSH, its values also were significantly lower among EMR-exposed rats on 70th PND when compared to the control group (Figure 13).

Morphometric analysis

The difference in seminiferous tubules diameters between the EMR-exposed and control rats was significant on the 1st and 21st PNDs and non-significant on PND 70.

Seminiferous tubular diameters showed a significant increase among the EMR-exposed group when compared to the control one on 1st and 21st PNDs; however, on 70th PND, the difference between EMR-exposed and control groups was non-significant. Regarding the interstitial space, a significant increase was recorded in all EMR-exposed groups. There was a significant decline in germinal epithelium thickness among PND 70 group, EMR-exposed groups when compared to control animals (Table 2).

Semen analysis

In the rats scarified on PND 70, the sperm count in the control group ranged from 40-60 million/ml with a mean value of 50.61 ± 6.171 , while EMR-exposed group the number of sperms decline significantly to 8-10 million/ml with a mean value of 9.04 ± 0.515 .

The abnormal sperm forms' percentage in the control group (PND 70) ranged from 5.73% to 10.1% with a mean value of 7.54 ± 1.657 , whereas in the EMR-exposed group (PND 70) the levels significantly elevated to reach 22 % to 28.1 % with a mean value of 25.20 ± 2.295 .

In the control group (PND 70), the sperm motility percentage ranged from 80% to 90% with a mean of 84.74 ± 3.828 , however, the sperm motility percentage in the EMR-exposed group (PND 70), was lower compared to the control group reached 30% to 50% with a mean value of 38.99 ± 6.804 (Figure 14).

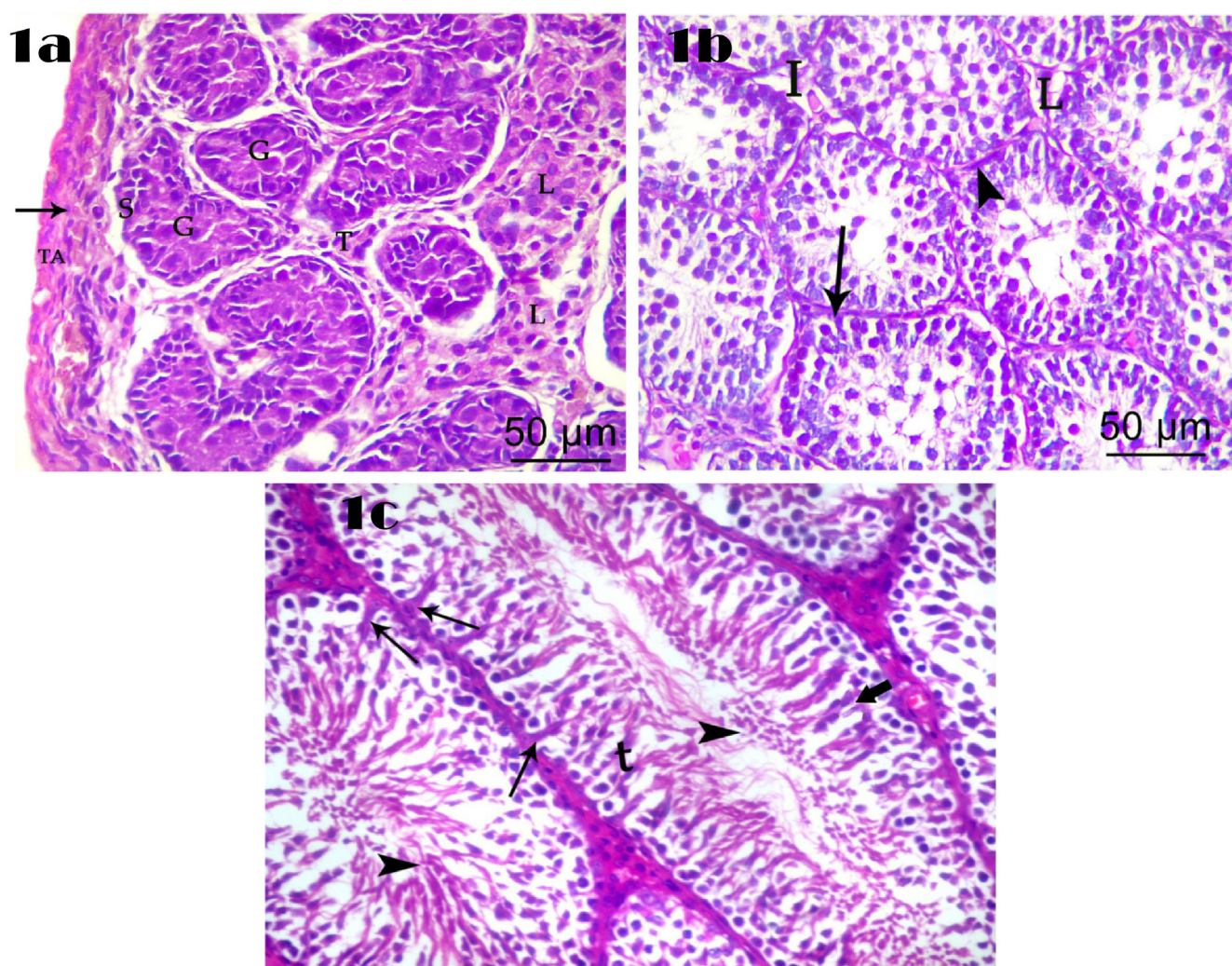


Fig. 1: Photomicrographs of sections of rat testis of the control subgroups showing: 1a) At the 1st PND, seminiferous cords appear surrounded with tunica albuginea (TA) which is formed of connective tissue and spindle shaped cells with deeply stained nuclei (arrow). The interstitial tissue (T) contains clusters of fetal Leydig cells (L).; 1b) At PND 21, seminiferous tubules show well-defined basal lamina (arrowhead), Sertoli cells (arrow) and spermatogenic cells (SP). The tubules are separated by narrow inter-tubular space (I) containing Leydig cells (L); 1c) At 70th PND, well developed seminiferous tubules are seen with Sertoli cells (arrows), spermatogenic cells (SP), spermatid (thick arrow) and acidophilic sperm (arrow heads). (H&E X 400)

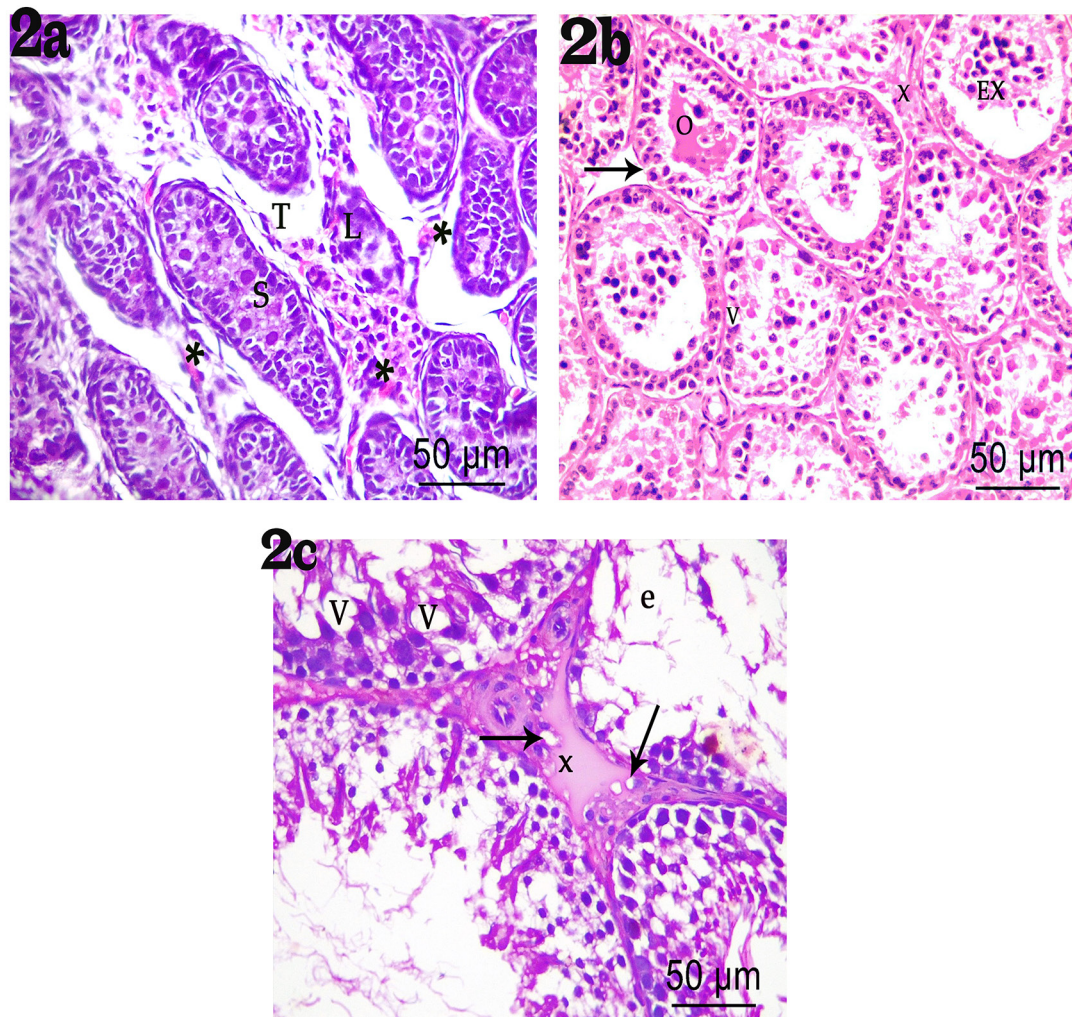


Fig. 2: Photomicrographs of sections of the rat testis of EMR-exposed groups showing: 2a) At the 1st PND, the seminiferous cords (S) appear widely separated (T). Mild congestion (*) and clustering of Leydig cells (L) are observed; 2b) At PND 21, seminiferous tubules appear with distorted basal lamina (arrow). Some exfoliated germ cell (EX) and deposition of homogenous acidophilic material (O) in their lumina. The seminiferous epithelium shows many vacuoles (V). Homogenous acidophilic material (X) deposition appears between the interstitial cells; 2c) At 70th PND, Seminiferous tubules have destructed lining epithelium (e) with vacuoles (V). Hyalinization (X) and some vacuoles (arrows) are seen in the interstitial space. (H&E X 400)

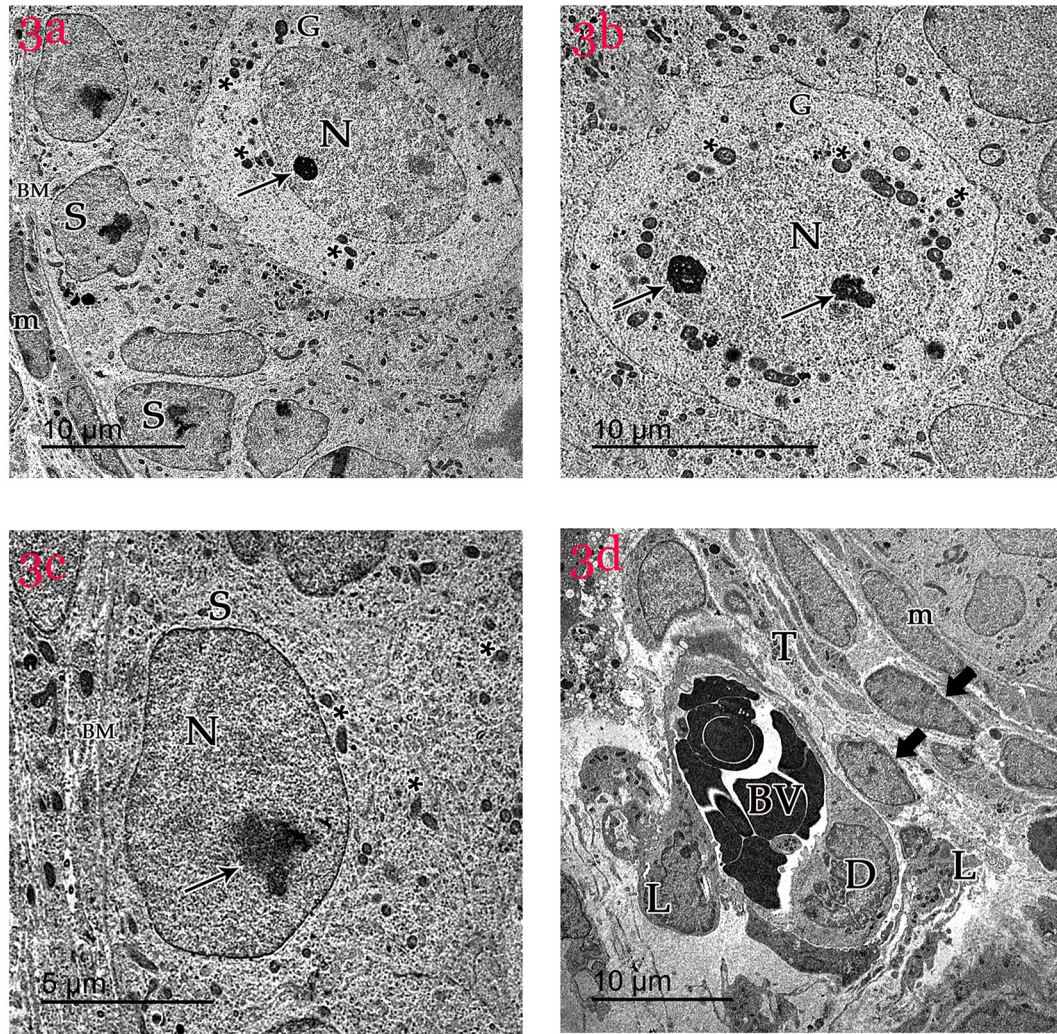


Fig. 3: Transmission electron micrographs of the rat testis of control groups at 1st PND showing: 3a) Part of seminiferous tubule surrounded by basement membrane (BM) and flat myoid cells (m). The tubule is lined with Sertoli cells (S) and gonocyte (G) lying near the center; 3b) Gonocytes (G) with spherical euchromatic nucleus (N) and prominent nucleolus (arrow). The cytoplasm has many mitochondria (*) with perinuclear arrangement; 3c) Sertoli cell (S) resting on basement membrane (BM) with oval euchromatic nucleus (N) and prominent nucleolus (arrow) are observed. The cytoplasm has many mitochondria (*); 3d) Interstitial space (T) contains: Leydig cells (L) and other undifferentiated mesenchymal cells (thick arrow) are seen near a blood vessel (BV) lined with endothelium (D). Flat myoid cells (m) are recognized. (3a: X2800; 3b: X4500; 3c: X6800; 3d: X 2800)

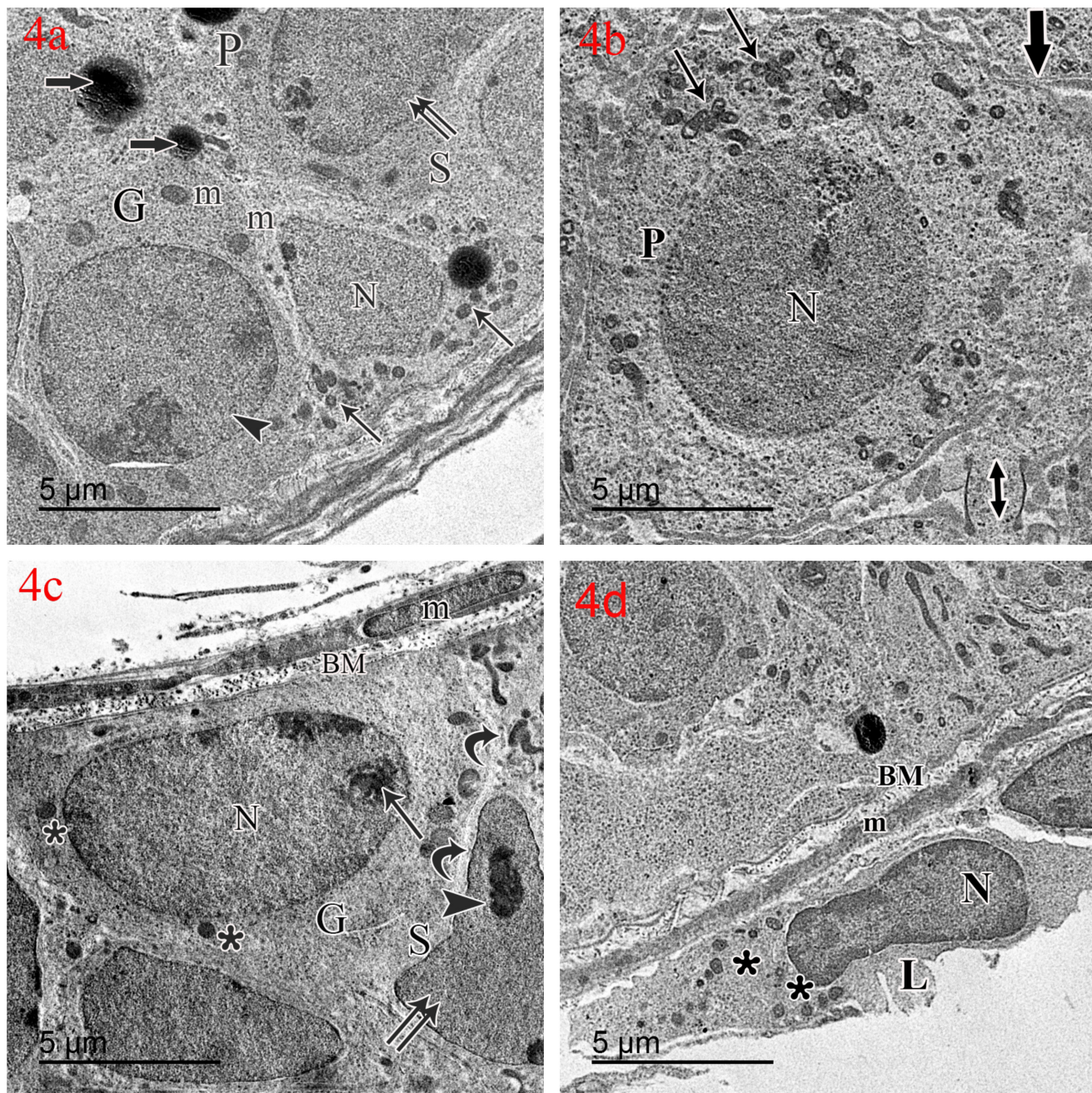


Fig. 4: Transmission electron micrographs of the rat testis of control groups at 21st PND showing: 4a) Part of seminiferous tubule lined with Sertoli cell (S), spermatogonia (G) with its spherical nucleus (arrow head) and primary spermatocyte (P) with its euchromatic nucleus (double arrow). Sertoli cell has pyramidal euchromatic nucleus (N) and many mitochondria (arrow). Some lysosomes can be observed (thick arrow); 4b) Primary spermatocytes (P) appear with large spherical euchromatic nucleus (N) and many mitochondria (arrows). Blood testis barrier (thick arrow) and inter cytoplasmic bridge (doubled arrow head) can be seen; 4c) Spermatogonia (G) with euchromatic nucleus (N), prominent nucleolus (arrowhead) and many mitochondria (*) are seen. Sertoli cells (S) has pyramidal nucleus (double arrows) with prominent nucleolus (arrowhead). Blood-testis barrier is seen (curved arrow); 4d) Intertubular space containing Leydig cell (L) with euchromatic nucleus (N) and mitochondria (*) appears. The basement membrane (BM) can be seen. (4a: X2800; 4b: X6800; 4c: X6800; 4d: X1500; 4e: X8500)

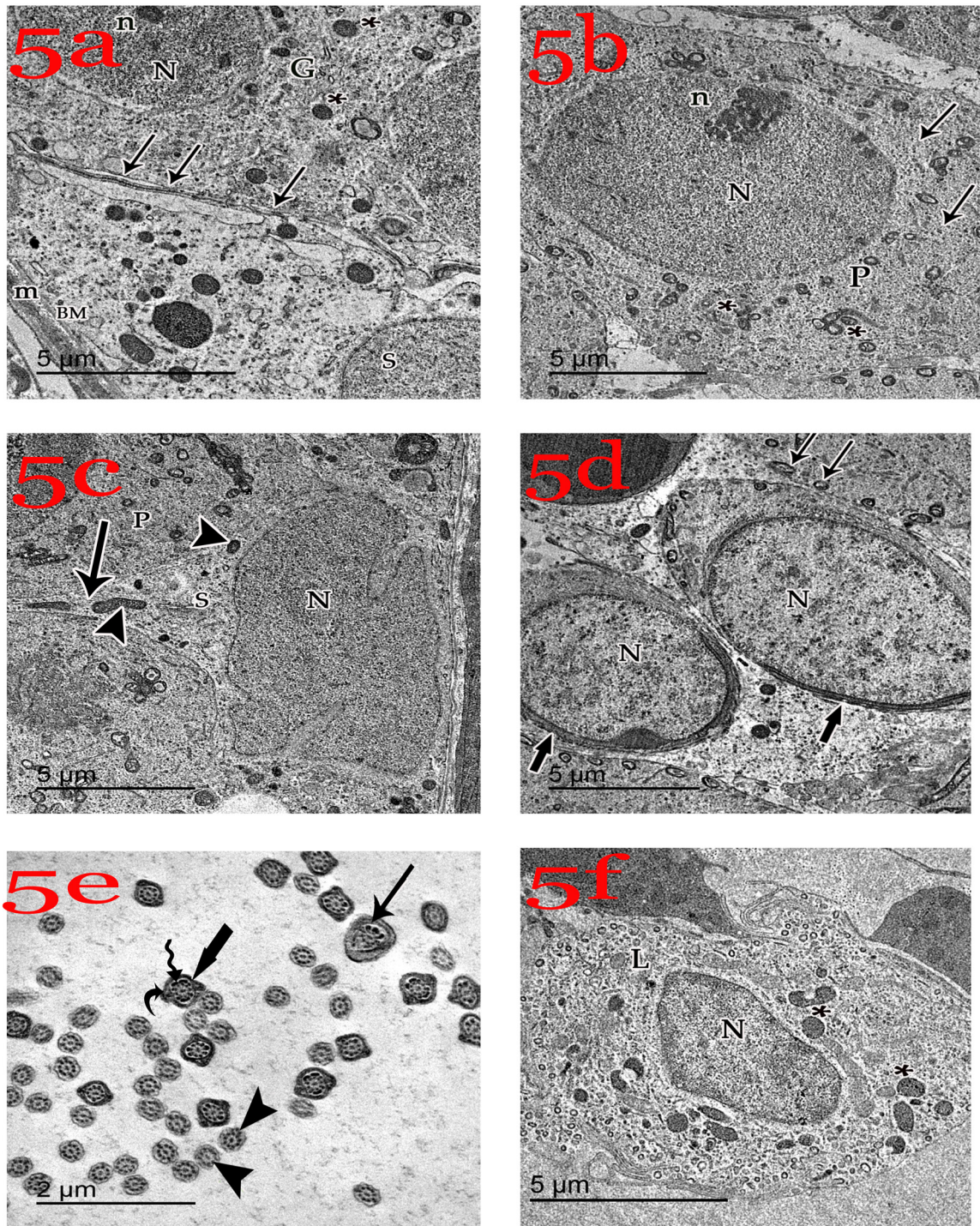


Fig. 5: Transmission electron micrographs of testes sections of control group at 70th PND showing: 5a) Spermatogonia (G) having euchromatic nucleus (N) with prominent nucleolus (n) and cytoplasm containing mitochondria (*) resting on basement membrane (BM) and flat myoid cells (m). Blood-testis barrier (arrows) is seen; 5b) Primary spermatocyte (P) has spherical euchromatic nucleus (N) with prominent nucleolus (n). Its cytoplasm contains many mitochondria (*) and free ribosomes (arrow); 5c) Sertoli cell (S) has euchromatic indented nucleus (N) and many mitochondria (arrowheads). The intracytoplasmic process of Sertoli (arrow) extends between primary spermatocytes (P); 5d) Spermatids with rounded euchromatic nucleus (N) and acrosomal cap (thick arrow) and acrosomal vesicle (double arrow) can be seen on one side of nucleus. The cytoplasm contains peripherally arranged mitochondria (arrows); 5e) Showing luminal part of germinal epithelium with cross sections in the principal piece (thick arrow); midpiece (arrows), and end piece (head arrow) of mature sperm. The principal piece is formed of nine doublets of microtubules (wavy arrow) with two central singlets enclosed by fibrous sheath (curved arrow). The end piece has nine doublets with two central singlets covered by cell membrane only (arrow head). 5f) Leydig cell (L) has euchromatic nucleus (N) and many mitochondria (*). (5a: X8500; 5b: X6800; 5c: X8500; 5d: X8500; 5e: X17000; 5f: X6800)

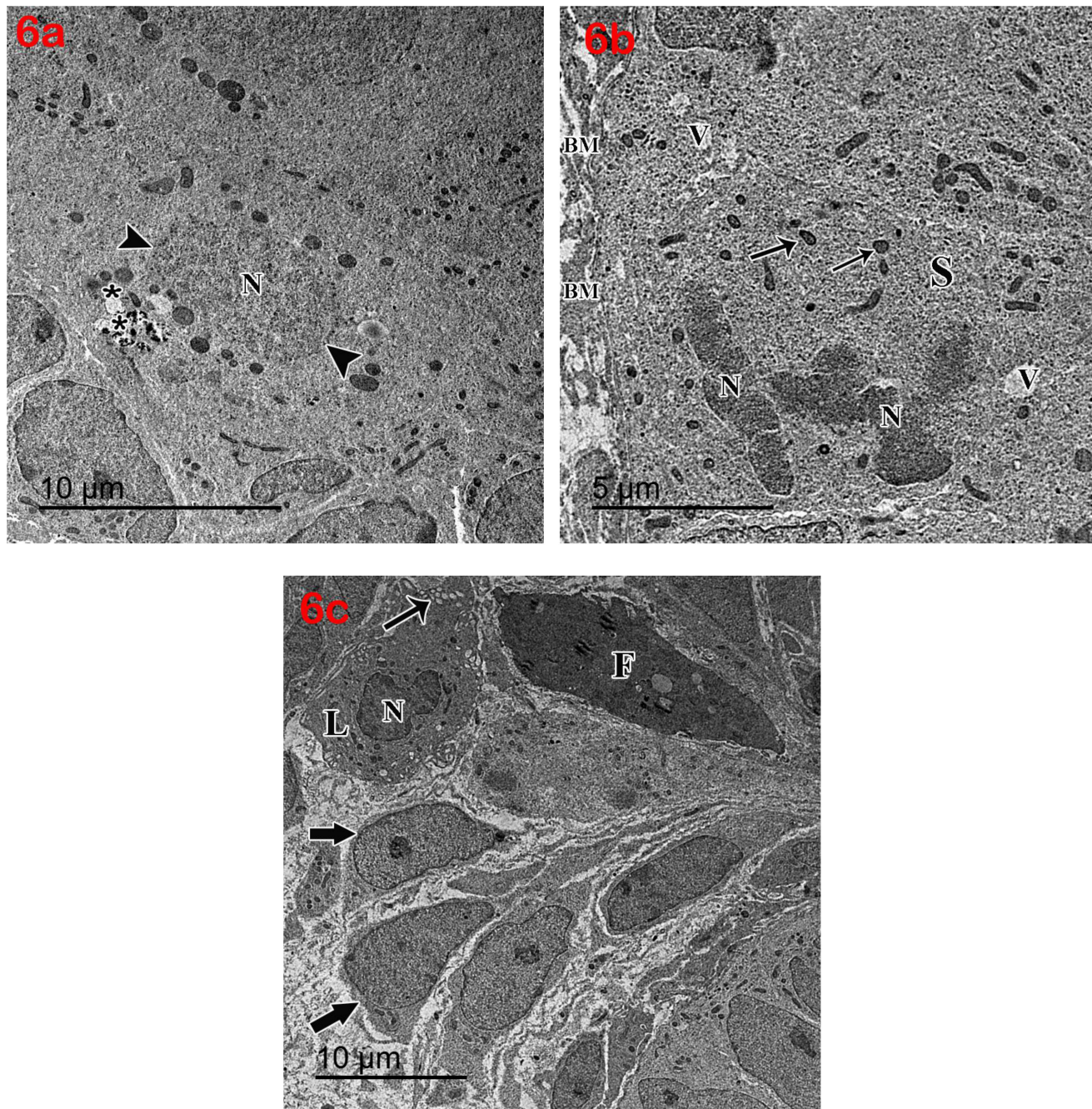


Fig. 6: Transmission electron micrographs of testes sections of EMR-exposed group at 1st PND showing: 6a) Gonocytes with absence of nuclear membrane (arrow heads), karyolysis of chromatin (N) and many cytoplasmic vacuoles (*); 6b) Sertoli cell (S) has completely fragmented nucleus (N), multiple vacuoles (v) and multiple mitochondria (arrow) in the cytoplasm rests on irregular basement membrane (BM); 6c) Leydig cells (L) with indented nucleus (N) and multiple vacuoles (arrows). Fibroblast-like cells (F) or undifferentiated mesenchymal cells (most probably) are also observed. (6a: X2800; 6b: X6800; 6c: X2800)

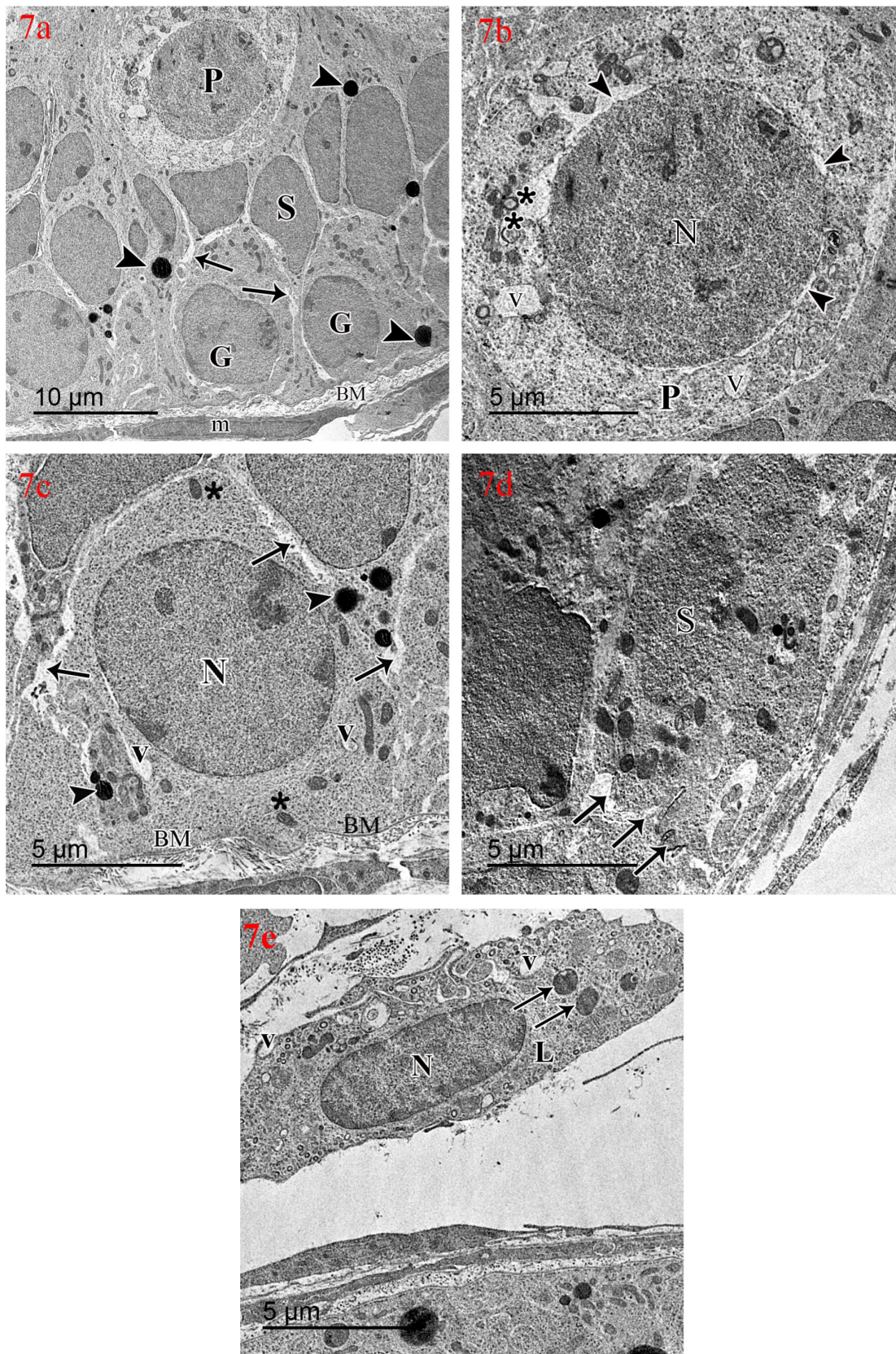


Fig. 7: Transmission electron micrographs of testes sections of EMR- exposed group at the 21st PND showing: 7a). Seminiferous tubule with irregular thickened basement membrane (BM) and (m) myoid cell. There are intercellular separations (arrows). The tubules are lined with spermatogonia (G), Sertoli cells (S) and primary spermatocytes (P) containing many lysosomes (arrow heads); 7b) Primary spermatocyte (P) showing spherical nucleus (N) with blebbing of nuclear membrane (arrow heads). Vacuoles are present in the cytoplasm (v); 7c) Spermatogonium appears resting on irregular basement membrane (BM) with peripheral euchromatic nucleus (N) and some vacuoles (v). Wide intercellular spaces (arrow) between spermatogenic cells can be seen ; 7d) Sertoli cell (S) showing disappearance of nuclear membrane and distorted blood-testis barrier (arrows) 7e) Leydig cell (L) has oval euchromatic nucleus with peripheral heterochromatin (N), and multiple vacuoles (v). (7a: X2800; 7b: X6800; 7c: X6800; 7d: X6800; 7e: X6800)

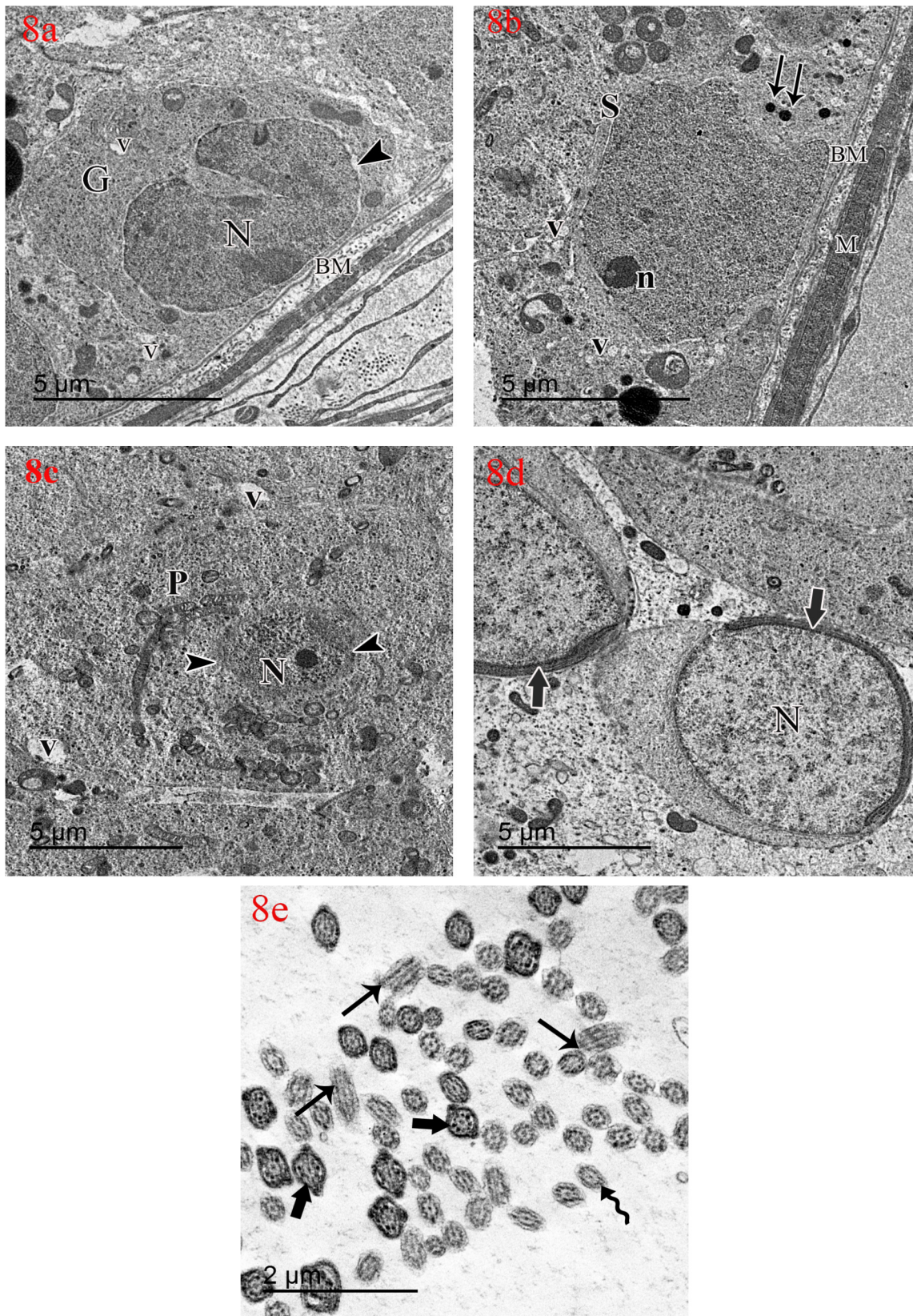


Fig. 8: Transmission electron micrographs of testes sections of EMR- exposed group at PND 70 showing: 8a) Spermatogonia (G) with irregular indented heterochromatic nucleus (N) and multiple cytoplasmic vacuoles (v) resting on thick basement membrane (BM); 8b) Sertoli cell (S) has euchromatic nucleus (N) with prominent nucleolus (n). Its cytoplasm has multiple vacuoles (v) and electron dense granules (arrows). Thickened basement membrane is noticed (BM); 8c) Degenerating primary spermatocytes (P) with condensed nuclear chromatin (N) and loss of nuclear envelop. Its cytoplasm has vacuoles (v); 8d) Abnormal spermatid with eccentric nucleus (N) and acrosomal cap (thick arrow). Peripheral mitochondria cannot be visualized; 8e) Cross sections in the tail of sperm showing disorganized midpiece (black arrows), principal piece (thick arrows) and end piece (wavy arrow). (8a: X8500; 8b: X8500; 8c: X6800; 8d: X8500; 8e: X17000)

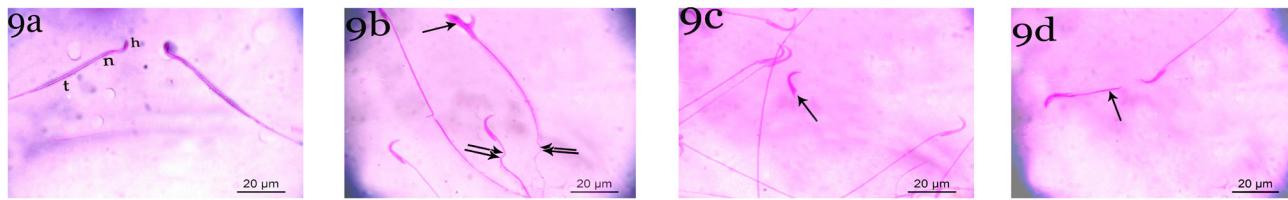


Fig. 9: Photomicrograph of rat sperms showing: 9a) Normal rat sperm at PND 70 showing normal head (h), neck (n) and tail (t); 9b) In the EMR- exposed group the sperm appears with broken head (arrow) and abnormal tail (double arrows); 9c) In the EMR- exposed group some sperms appear with detached part (arrow); 9d) In the EMR- exposed group also sperm has short tail (arrow). (Eosin-Nigrosin X1000)

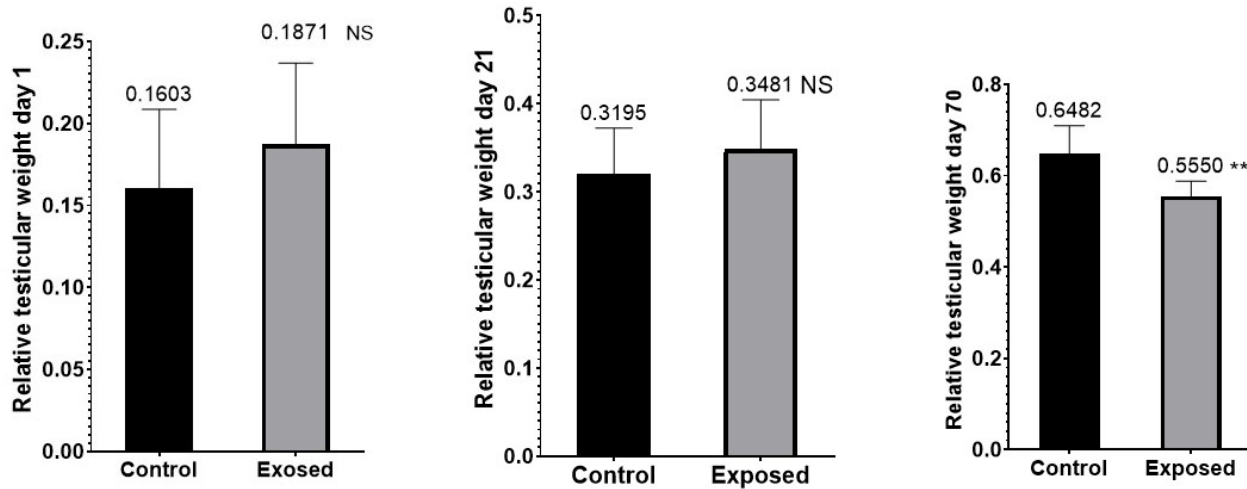


Fig. 10: Mean relative testicular weights of control and EMR-exposed rats. Bars represent the mean \pm SD of 20 replicates. Significant at P value less than 0.001, (Ns) indicates non-significant results.

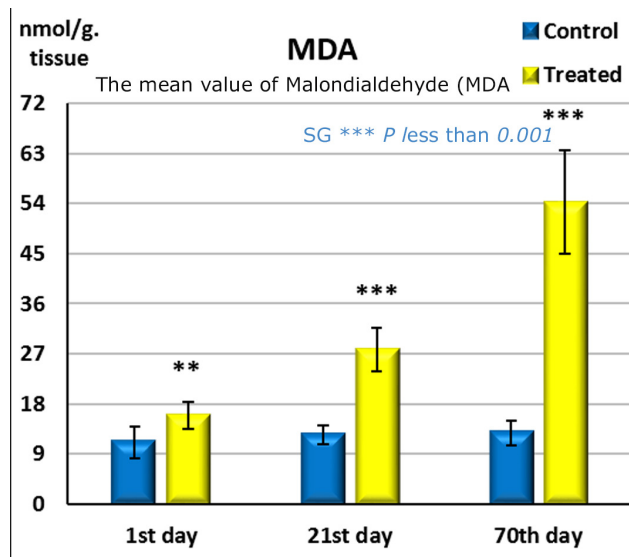


Fig. 11: Bar chart showing the mean value of malondialdehyde (MDA) in in all studied groups Significant (***) at P value less than 0.001, (Ns) indicates non-significant results.

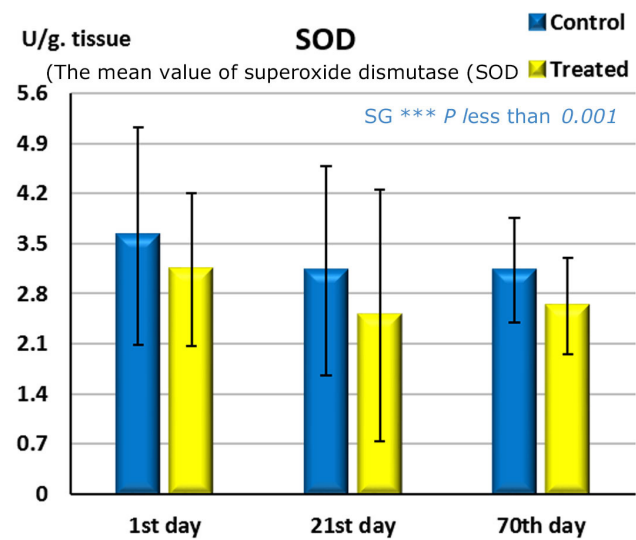


Fig. 12: Bar chart showing the mean value of superoxide dismutase (SOD) in all studied groups Significant (***) at P value less than 0.001, (Ns) indicates non-significant results.

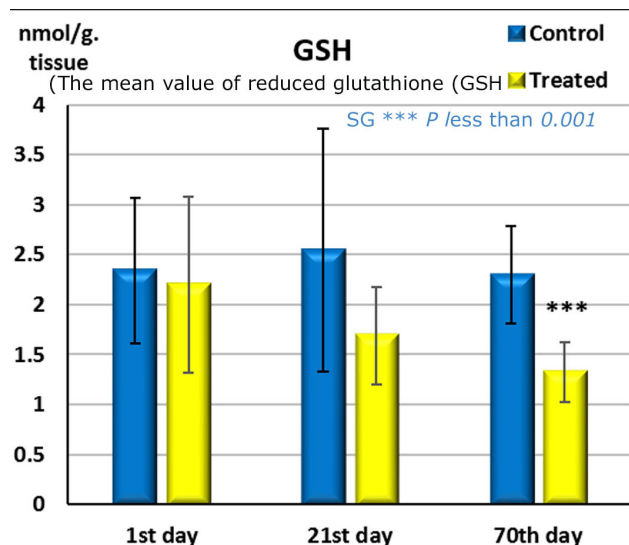


Fig. 13: Bar chart showing the mean value of reduced glutathione (GSH) values in all studied groups Significant (***) at P value less than 0.001, (Ns) indicates non-significant results.

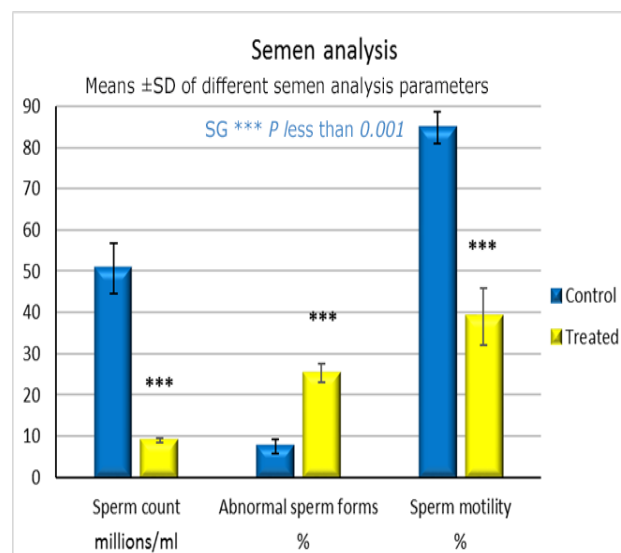


Fig. 14: Bar chart showing means ±SD of different semen analysis parameters in different studied groups at PND 70. Significant (***) at P value less than 0.001, (Ns) indicates non-significant results

Table 1: Effects of EMR- Exposure on offspring's body weight, absolute, and relative testicular weights

Parameter	1 st day		21 st day		70 th day	
	Control group	EMR-exposed group	Control group	EMR-exposed group	Control group	EMR-exposed group
Total body weight (gm)	6.68 ± 0.512	5.51 ± 0.557 ^{***}	31.88 ± 5.384	32.50 ± 5.043 ^{Ns}	65.75 ± 4.400	54.63 ± 3.926 ^{***}
Absolute Testis weight (mg)	10.63 ± 2.925	10.50 ± 2.449 ^{Ns}	100.30 ± 16.25	111.50 ± 12.73 ^{Ns}	428.30 ± 33.29	302.9 ± 17.67 ^{***}
Relative testicular weight	0.160 ± 0.0482	0.187 ± 0.0496 ^{Ns}	0.319 ± 0.0528	0.3481 ± 0.0564 ^{Ns}	0.648 ± 0.0615	0.555 ± 0.0334 ^{***}

All values are expressed as mean ±SD, the results were considered statistically significant when the *P* value < 0.05; Significant (***), (Ns) indicates non-significant results

Table 2: Effects of EMR- Exposure on Seminiferous tubule diameter, Interstitial space and Germinal epithelium thickness

Parameter	1 st day		21 st day		70 th day	
	Control group	EMR-exposed group	Control group	EMR-exposed group	Control group	EMR-exposed group
Seminiferous tubule diameter (µm)	35.97 ± 4.190	44.12 ± 4.383 ^{**}	49.79 ± 5.459	69.30 ± 4.404 ^{***}	128.5 ± 5.091	123.1 ± 9.618 ^{Ns}
Interstitial space (µm)	7.69 ± 2.134	13.19 ± 2.165 ^{***}	5.12 ± 1.470	12.99 ± 3.777 ^{***}	5.44 ± 1.086	17.75 ± 6.450 ^{***}
Germinal epithelium thickness (µm)		No data The tubules are not canalized yet			39.07 ± 6.040	25.15 ± 2.664 ^{***}

All values are expressed as mean ±SD, the results were considered statistically significant when the *P* value < 0.05; Significant (***), (Ns) indicates non-significant results

DISCUSSION

Continuous postnatal changes of male gonads make them prone to environmental hazards. The current study investigated testicular changes associated with EMR body exposure using a rat model. Rats were chosen as experimental animals because they have biological similarities to humans. Besides, the rodents develop diseases over a span of days or weeks instead of months or years. Furthermore, their fertility is susceptible to a variety of agents as inhuman, albeit the output of human sperms is approximately four times less than other mammals^[24]. The reasoning for employing 20 min full-power radiation was simply the routine use of cell phones in our daily lives^[12].

In rats, the first wave of spermatogenesis, occurring from the first to seventh weeks of postnatal life, is the key process in sexual maturation. That makes the prepubertal stage much more sensitive to testicular alteration by an environmental toxin^[25]. It has been suggested that EMR emitted from mobile phones leads to DNA damage to human spermatozoa^[26]. In the current study, EMR emitted from a cell phone was applied to pregnant rats, so the pups were exposed to radiation effect in the prenatal period and continued in the postnatal period. No analysis was performed on the mothers. In the present work light, microscopic examination of the control group on 1st PND showed solid seminiferous tubules. This observation follows Picut *et al.*,^[27] who stated that the canalization of the seminiferous tubules occurs by postnatal day 18.

The most prominent finding on PND1 of control rats was the presence of gonocytes occupying the central portion of the cords which is parallel to Kleymenova *et al.*,^[28] who stated that the newborn testis is formed of solid cords with two main cell types which are differentiable: the most numerous cells are the Sertoli cells, and the second type is gonocytes. Another intriguing finding was the presence of intercellular bridges between the spermatogenic cells. Germ cells have large (0.5-3µm), constant, intercellular communication which are wide enough to allow the passage of mitochondria^[29].

As regards EMR exposure in this age group, the seminiferous tubules appeared widely separated. According to another study^[13], such widening of peritubular space was attributed to spermatogenesis impairment. Other studies stated that the EMR exposure interferes with the endocrine regulation of spermatogenesis followed by withdrawal of gonadotrophic stimulation which may explain this peritubular widening^[30].

On examination of ultrathin sections of testis of the same age, gonocytes had disintegrated nuclear membrane and karyolysis of nuclear chromatin. As well, Sertoli cells appeared with multiple fragmented nuclei. This finding is following the observations of Almášiová *et al.*^[1] who detected disrupted mitochondria and electron-dense granules in the cytoplasm of Sertoli cells. In addition, fibroblast-like undifferentiated mesenchymal cells have been seen in the peritubular spaces. A previous study^[31] explained that Leydig cells differentiation passes through different stages postnatally; the early identifiable cells appear as undifferentiated fibroblast-like cells that act as a precursor cell to adult Leydig cells.

LM examination of EMR-exposed animals of the PND 21 group showed distorted seminiferous tubules, exfoliation of germinal cells into lumen. Some literature mentioned that the presence of exfoliated cells could be explained by the disruption in the connection between the Sertoli cells and differentiating germ cells^[32]. The study of Rai *et al.*^[33] attributed this observation to the reduction of the germ cells number and the subsequent retraction of the cytoplasmic processes of the Sertoli cells so that cells became loosely arranged and easily sloughed out. Moreover, the presence of homogenous acidophilic material in some tubules could be attributed to the deterioration of phagocytic activity of Sertoli cells^[13].

At the ultrastructural level, the EMR-exposed group, on PND 21, showed spermatogonia with many cytoplasmic vacuoles resting on a thick basement membrane. Sertoli cells lost their nuclear membrane with discontinuity of blood-testis- barrier. The previous findings were formerly reported by Almášiová *et al.*^[1] who found that rats exposed to EMR 3h daily for 3 weeks had empty spaces between Sertoli cells and spermatogonia in addition to multiple vacuoles within primary spermatocytes.

On PND 70, the results of light microscopic study are the same as those showed by Lee *et al.*,^[34] and Tenorio

et al.,^[35] who reported that exposure to EMR resulted in a reduction in the number of well-organized seminiferous tubules, vacuolation of epithelium, increase in germ cell death and arrest of spermatogenesis. The vacuoles seen in the germinal epithelial lining of EMR-exposed pups possibly is a result of hydropic degeneration as cells accumulate much water due to mitochondrial dysfunction^[36].

In ultrathin sections, the vacuoles were also present in the cytoplasm of some Sertoli cells. According to Wong *et al.*^[37], vacuoles in Sertoli cells may come from the accumulation of lipid droplets used for nourishing germ cells. The swollen perinuclear space of Sertoli cells was also noticed by Tenorio *et al.*,^[35]. Additionally, the basement membrane of the seminiferous tubules showed thickening and irregularity. The presence of an exogenous stimulant may induce myoid cells to produce more collagen and extracellular matrix that could impair spermatogenesis^[38,39].

In the current work, there was no significant difference either in the absolute or in the relative weight of the testis between the control and exposed groups on PND 1 and 21. In contrast, both the absolute and relative testicular weights were significantly lower in the exposed group on PND 70 when compared with the control one. This coincides with the study of Odaci *et al.*^[40] who found a significance reduction in the weight of testis on PND 60 after intrauterine exposure to 900 MHz electromagnetic field. Meanwhile, the total body weight was lower in exposed groups on PNDs 1 and 70. The previous results are in agreement with Ozunger *et al.*^[41] who reported no change in testis weights in rats exposed to 900 MHz for 30 min/day, 4 times per week for 5 weeks.

In the same line, the results of the current study showed that EMR waves had adversely changed the redox status in the testicular tissue through the induction of oxidative stress and concomitant disruption of the testicular antioxidant system. MDA is an important indicator of lipid peroxidation that determines oxidative stress status, so its high level reflects this clinical situation^[42]. The current study revealed that MDA levels were significantly higher in all EMR- exposed groups (PNDs 1, 21, and 70) when compared to the corresponding control ones.

Mobile waves can generate destructive ROS, including superoxide, hydrogen peroxide, and hydroxyl radical, frequently result in oxidative damage and histological changes^[43]. ROS are continuously neutralized by antioxidants present in body tissues. Some studies have shown that oxidative stress develops in response to cell phone radiation. EMR may disturb ROS metabolism by increasing their production or by decreasing the activity of antioxidant enzymes^[13]. SOD plays a central role in defending against oxygen free radicals by eliminating nitrous oxide and prevention peroxynitrite production (Fukai *et al.* 2011.^[44] Reduced glutathione (GSH) is a potent thiol antioxidant in living tissues. As it restores redox status forms glutathione disulfide then reduced again by glutathione reductase, It functions as a recyclable antioxidant., Gong, 2017^[45] The present study revealed

that SOD activity and GSH level were significantly lower among the exposed rats when compared to control groups.

The capability of EMR to induce oxidative stress in the testes strongly suggests that the testis is a vulnerable tissue that is highly dependent on oxygen to drive spermatogenesis and yet highly susceptible to toxic effects of reactive oxygen metabolites^[13].

The previous findings were supported by a morphometric analysis which revealed that the seminiferous tubule diameter was significantly higher in rats exposed cell phone radiation, in groups PND 1 and 21 but not in group PND 70. Other authors did not observe a significant difference from exposure of rats to 220 MHz pulsed modulated RF for one month^[46], electromagnetic field of 2 cell phones for 3 months^[47], and to 900 MHz radiofrequency radiation for one year^[48].

The seminiferous epithelial thickness decreased significantly among exposed rats in PND 70 group. However, there was no significant difference in thickness among exposed groups in PND 1 and 21 groups. These results are supported by the findings of Tenorio *et al.*^[35] who investigated the effect of EMR exposure in utero and postnatally till the PND 90, and Al-Damegh^[49] who studied the effect of cell phone on adult rats explaining that radiation harms testicles through the induction of oxidative stress with concomitant disruption of the testicular antioxidant status. Ozguner *et al.*^[39] mentioned a reduction in both seminiferous tubules diameter and their epithelial thickness in rats exposed to RF-EMW of 869 to 894 MHz.

Concerning sperm count in the current study, it was significantly low in EMR-exposed groups in comparison with the controls. Also, the abnormal sperm forms and total sperm motility percentage were significantly higher in the same group when compared with control rats of corresponding age. The use of cell phones decreased the semen quality in men by decreasing the sperm counts, motility, viability, and normal morphology^[50]. In the same line, exposure of rats to EMR for 30 min per day three times per week for 2 weeks or to acute dose, 3h of a magnetic field, caused germ cell degeneration, slowed spermatogenesis, reduced the daily sperm production, and affected sperm motility and morphology^[51]. In contrast, Yan *et al.*^[52] did not report any adverse effect of cell phone exposure on sperm count, morphology, or motility in the rats.

CONCLUSION

Cell phones might have serious consequences on the developing testis, especially in the early stages of life. Therefore, it is recommended to minimize the daily exposure to such appliances, especially for pregnant women and males before puberty.

ABBREVIATIONS

BTB: blood-testis barrier; **EM:** Electron microscopy; **EMF:** Electromagnetic fields; **EMR:** Electromagnetic radiation; **GSH:** Glutathione; **GSM:** global system

for mobile; **H&E:** Hematoxylin and Eosin; **LM:** light microscopy; **MDA:** Malondialdehyde; **NS:** Non-significant; **PND:** Postnatal day; **RF:** Radiofrequency; **ROS:** Reactive oxygen species; **SAR:** Specific absorption rate; **SD:** Standard deviation; **SOD:** Superoxide dismutase.

CONFLICT OF INTERESTS

There are no conflicts of interest.

REFERENCES

1. Almášiová V, Holovská K, Cigánková V, Račková E, Fabianová K, Martončíková M. Structural and ultrastructural study of rat testes influenced by electromagnetic radiation. *J Toxicol Environ Health A.* (2014); 77.13:747-50.
2. Swerdlow AJ, Feychting M, Green AC, Kheifets L, Savitz DA. International Commission for Non-Ionizing Radiation Protection Standing Committee on Epidemiology. Mobile phones, brain tumors, and the interphone study: where are we now? *Environ Health Perspect.* (2011);119.11:1534-8.
3. Özorak A, Nazıroğlu M, Çelik Ö, Yüksel M, Özçelik D, Özkaya MO, Çetin H, Kahya MC, Kose SA. Wi-Fi (2.45 GHz) and mobile phone (900 and 1800 MHz)-induced risks on oxidative stress and elements in kidney and testis of rats during pregnancy and the development of offspring. *Biol Trace Elem Res.* (2013);156(1-3): 221-9.
4. Djeridane Y, Touitou Y, De Seze R. Influence of electromagnetic fields emitted by GSM-900 cellular telephones on the circadian patterns of gonadal, adrenal, and pituitary hormones in men. *Radiation Research.* (2008); 169.3:337-43.
5. Alchalabi AS, Aklilu E, Aziz AR, Malek F, Ronald SH, Khan MA (2016) Different periods of intrauterine exposure to the electromagnetic field: Influence on female rats' fertility, prenatal and postnatal development. *Asian Pacific J Reprod.* 5.1:14-23.
6. Hardell L, Carlberg M, Mild KH. Use of mobile phones and cordless phones is associated with increased risk for glioma and acoustic neuroma. *Pathophysiology.* (2013); 20.2:85-110.
7. Ochiogu IS, Uchendu CN, Ihedioha JI. A new and simple method of confirmatory detection of mating in albino rats (*Rattus norvegicus*). *Animal Research International.* (2006); 3.3:527-30.
8. Sephehrimanesh M, Kazemipour N, Saeb M, Nazifi S. Analysis of rat testicular proteome following 30-day exposure to 900 MHz electromagnetic field radiation. *Electrophoresis.* (2014); 35.23:3331-8
9. Hancı H, Odacı E, Kaya H, Aliyazıcıoğlu Y, Turan İ, Demir S, Çolakoğlu S. The effect of prenatal exposure to 900-MHz electromagnetic field on the 21-old-day rat testicle. *Reprod Toxicol.* (2013); 42:203-9.

10. Kesari KK, Behari J. Evidence for mobile phone radiation exposure effects on reproductive pattern of male rats: role of ROS. *Electromagnetic biology and medicine.* ((2012); 31.3:213-22.
11. Poulletier de Gannes F, Haro E, Hurtier A, Taxile M, Athane A, Ait-Aissa S, Masuda H, Percherancier Y, Ruffié G, Billaudel B, Dufour P. Effect of in utero Wi-Fi exposure on the pre- and postnatal development of rats. *Birth Defects Res B Dev Reprod Toxicol.* (2012); 95.2:130-6.
12. Uslu BA, Kilic DK, Gulyuz F, Deger Y, Ucar Ö. Effect of electromagnetic wave emitted from mobile phone on some reproductive parameters in adult male guinea pigs. *Atatürk Üniversitesi Vet Bil Derg.* (2012); 7.2:77-84.
13. Farag, Eman Abas, and Marwa Mohamed Yousry. "Effect of mobile phone electromagnetic waves on rat testis and the possible ameliorating role of Naringenin: A histological study." *Egyptian Journal of Histology* (2018); 41.1 :108-121.
14. Hegazy R, Hegazy A . Hegazy'Simplified Method of Tissue Processing (Consuming Less Time and Chemicals). *Annals of International Medical and Dental Research.* (2015); 1.2:57-61.
15. Woods AE, Stirling JW. Transmission electron microscopy applications. In: Layton C, Bancroft JD, editors. *Theory and practical histological techniques.* Ch 22, 7th ed. Philadelphia, Churchill Livingstone, (2013); pp 493 – 538.
16. Ohkawa H, Ohishi N, Yagi K. Assay for lipid peroxides in animal tissues by thiobarbituric acid reaction. *Anal Biochem.* ((1979); 95.2: 351-8.
17. MacCord JM. Superoxide dismutase: an enzymatic function for erythrocyte (hemocuprein). *J. Biol. Chem.* ((1969); 244:6049-55.
18. Tietze F. Enzymic method for quantitative determination of nanogram amounts of total and oxidized glutathione: applications to mammalian blood and other tissues. *Analytical biochemistry.* (1969);27.3: 502-522.
19. Jamall IS, Smith JC Effects of cadmium on glutathione peroxidase, superoxide dismutase, and lipid peroxidation in the rat heart: a possible mechanism of cadmium cardiotoxicity. *Toxicology and Applied Pharmacology.* (1985); 80.1:33-42.
20. Yokoi K., Uthus EO., Nielsen FH. Nickel deficiency diminishes sperm quantity and movement in rats. *Biol. Trace. Elem. Res.* (2003); 93, 141-153
21. Noakes DE and DJ. Parkison . "Arther's. *Veterinary Reproduction and Obstetrics*". 8th ed Gary Cw England (2001).
22. Sonmez M., Turk G., Yuce A., The effect of ascorbic acid supplementation on sperm quality, lipid peroxidation and testosterone levels of male Wistar rats. *Theriogenology,* , (2005); 63:2063-2072.
23. Atessahin A., Karahan I., Turk G., Gur S., Yilmaz S., Ceribasi AO., Protective role of lycopene on cisplatin induced changes in sperm characteristics, testicular damage and lipid peroxidation in rats. *Reprod. Toxicol.,* (2006); 21: 42-47
24. Amann RP, Howards SS. Daily spermatozoal production and epididymal spermatozoal reserves of the human male. *J Urol.* (1980) ;124.2:211-5.
25. Kondo T, Shono T, Suita S. Age-specific effect of phthalate ester on testicular development in rats. *Journal of pediatric surgery.* (2006); 41.7:1290-3.
26. Kumar P, Shukla V. Ultrastructural changes in rat testicular tissue after whole body exposure to electromagnetic radiation emitted from mobile phones. *Journal of International Academic Research for Multidisciplinary.* (2014);2.1:518-26.
27. Picut, Catherine A., *et al.* "Postnatal development of the testis in the rat: morphologic study and correlation of morphology to neuroendocrine parameters." *Toxicologic pathology* (2015); 43.3: 326-342.
28. Kleymenova, Elena, *et al.* "Exposure in utero to di (n-butyl) phthalate alters the vimentin cytoskeleton of fetal rat Sertoli cells and disrupts Sertoli cell-gonocyte contact." *Biology of reproduction* (2005); 73.3: 482-490.
29. Greenbaum, Michael P., *et al.* "Germ cell intercellular bridges." *Cold Spring Harbor perspectives in biology* 3.8 (2011): a005850.
30. Agarwal A, Singh A, Hamada A, Kesari K. Cell phones male infertility: a review of recent innovations in technology consequences. *Int Bra J Urol.* (2011); 37: 432-54.
31. Chamindrani Mendis-Handagama, S. M. L., and H. B. Siril Ariyaratne. "Differentiation of the adult Leydig cell population in the postnatal testis." *Biology of reproduction* 65.3 (2001): 660-671.
32. Weyden VD, Arends MJ, Chausiaux OE. Loss of TSLC1 causes male infertility due to a defect at the spermatid stage of spermatogenesis. *Molecular and Cellular Biology* 2006; 26: 3595–609.
33. Rai J, Pandey SN, Srivastava RK. Effect of immobilization stress on spermatogenesis of albino rats. *J Anat Soc India.* (2003); 52.1:55-7.
34. Lee JS, Ahn SS, Jung KC, Kim YW, Lee SK. Effects of 60 Hz electromagnetic field exposure on testicular germ cell apoptosis in mice. *Asian Journal of Andrology.* (2004); 6.1:29-34.
35. Tenorio BM, Jimenez GC, de Moraes RN, Peixoto CA, de Albuquerque Nogueira R, da Silva VA. Evaluation of testicular degeneration induced by low-frequency electromagnetic fields. *J Appl Toxicol.* (2012);32.3: 210-8.

36. Levine S, Saltzman A, Ginsberg SD. Vacuolar pathology in the median eminence of the hypothalamus after hyponatremia. *Journal of Neuropathology & Experimental Neurology*. (2011); 70.2:151-6.
37. Wong CH, Cheng CY. The blood-testis barrier: its biology, regulation, and physiological role in spermatogenesis. *Current topics in developmental biology*. (2005) Jan 1; 71: 263-96.
38. Khalaf HA, Arafat EA, Ghoneim FM. A histological, immunohistochemical and biochemical study of the effects of pomegranate peel extracts on gibberellic acid induced oxidative stress in adult rat testes. *Biotechnic & Histochemistry*. (2019); 26:1-4.
39. Skinner MK. Cell-cell interactions in the testis. *Endocrine Reviews*. (1991);12.1:45-77.
40. Odacı, E., H. Hancı, E. Yuluğ, S. Türedi, Y. Aliyazıcıoğlu, H. Kaya, and S. Çolakoğlu. "Effects of prenatal exposure to a 900 MHz electromagnetic field on 60-day-old rat testis and epididymal sperm quality." *Biotechnic & Histochemistry* 91, no. 1 (2016): 9-19.
41. Ozguner M, Koyu A, Cesur G, Ural M, Ozguner F, Gokcimen A, Delibas N Biological and morphological effects on the reproductive organ of rats after exposure to electromagnetic field. *Saudi medical journal*. (2005);26.3: 405-10.
42. Ayala, A., Muñoz, M.F. and Argüelles, S., 2014. Lipid peroxidation: production, metabolism, and signaling mechanisms of malondialdehyde and 4-hydroxy-2-nonenal. *Oxidative medicine and cellular longevity*, 2014.
43. Khaki AA, Zarrintan S, Khaki A, Zahedi A. The effects of electromagnetic field on the microstructure of seminal vesicles in rat: a light and transmission electron microscope study. *Pakistan journal of biological sciences: PJBS*. (2008);11.5:692-701.
44. Fukai, Tohru, and Masuko Ushio-Fukai. "Superoxide dismutases: role in redox signaling, vascular function, and diseases." *Antioxidants & redox signaling* 15, no. 6 (2011): 1583-1606.
45. Gong, Zh., Tian, Gl., Huang, Qw. *et al.* Reduced glutathione and glutathione disulfide in the blood of glucose-6-phosphate dehydrogenase-deficient newborns. *BMC Pediatr* 17, 172 (2017).
46. Guo L, Lin JJ, Xue YZ, An GZ, Zhang JP, Zhang KY, He W, Wang Hb, Li W, Ding GR. Effects of 220 MHz Pulsed Modulated Radiofrequency Field on the Sperm Quality in Rats. *Int J Environ Res Public Health*. (2019);16.7:1-12.
47. Çelik, Serkan, I. Atilla Aridogan, Volkan Izol, Seyda Erdoğan, Sait Polat, and Şaban Doran. "An evaluation of the effects of long-term cell phone use on the testes via light and electron microscope analysis." *Urology* 79, no. 2 (2012): 346-350
48. Tas, Muzaffer, Suleyman Dasdag, Mehmet Zulkuf Akdag, Umut Cirit, Korkut Yegin, Ugur Seker, Mehmet Ferit Ozmen, and Leyla Bilge Eren. "Long-term effects of 900 MHz radiofrequency radiation emitted from mobile phone on testicular tissue and epididymal semen quality." *Electromagnetic biology and medicine* 33, no. 3 (2014): 216-222
49. Al-Damegh MA. Rat testicular impairment induced by electromagnetic radiation from a conventional cellular telephone and the protective effects of the antioxidants vitamins C and E. *Clinics (Sao Paulo)*. (2012); 67.7:785-92.
50. Agarwal A, Deepinder F, Sharma RK, Ranga G, Li J. Effect of cell phone usage on semen analysis in men attending infertility clinic: an observational study. *Fertil Steril*. (2008); 89.1:124-8.
51. Ramadan LA, Abd-Allah AR, Aly HA, Saad-El-Din AA. Testicular toxicity effects of magnetic field exposure and prophylactic role of coenzyme Q10 and L-carnitine in mice. *Pharmacological research*. (2002); 46.4:363-70.
52. Yan, Ji-Geng, *et al.* "Effects of cellular phone emissions on sperm motility in rats." *Fertility and sterility* (2007); 88.4: 957-964.

المخلص العربي

التعرض ما قبل الولادة وبعدها لإشعاع الهاتف الخليوي وتأثيره المحتمل على تطور أنسجة الخصية في الجرذان البيضاء دراسة بالمجهر الضوئي والمجهر الإلكتروني

عبد المنعم عوض حجازي، مروة محمود أحمد، نهى عبد المطلب، جوزيف امين عزيز
قسم التشريخ والأجنة- كلية الطب البشرى-جامعة الزقازيق

خلفية البحث : فترات ما حول الولادة هي مراحل حاسمة في تطور الخصية. والخصية هي عضو حساس شديد التأثير بالملوثات البيئية المحيطة و قد يكون التعرض للهواتف المحمولة وما ينتج عنها من أشعاع كهرومغناطيسي أحد أهم هذه الملوثات.

الهدف من البحث: صُممت هذه الدراسة لتقييم تأثير التعرض لإشعاعات الهاتف الخليوي قبل الولادة وبعدها على نمو خصيتي الجرذان

المواد والطرق المستخدمة: تم استخدام ستة عشر أنثى من الجرذان البيضاء. تعرضت الأمهات في المجموعة الثانية للهاتف الخليوي لمدة ساعتين / يوم من اليوم السادس من الحمل ، طوال فترة الرضاعة وحتى الفطام. استخدمنا أيضاً مجموعة اخرى من الأمهات كمجموعة ضابطة لم يتم تعريضها لأي إشعاع. تم تقسيم الذكور من كلتا المجموعتين إلى ثلاث مجموعات (تحتوى كل منها على ١٠ جرذان صغيرة) ؛ حسب اعمارهم وقت الذبح تم تقسيمهم كالآتى. المجموعة الفرعية الأولى A (تم الذبح في اليوم الأول من الولادة) و المجموعة الفرعية الثانية B (تم الذبح في اليوم الحادى والعشرين من الولادة) و المجموعة الفرعية الثالثة C (تم الذبح في اليوم السابعين من الولادة) ثم تم استئصال الخصيتين ومعالجتها للفحص بالمجهر الضوئي والمجهر الإلكتروني. و تم إجراء تقييم لعوامل الأكسدة والتحليل المورفومتري بالإضافة إلى تحليل السائل المنوي لكل مجموعة

النتائج: لوحظت تغيرات تنكسية مختلفة في بنية خصية الجرذان في الحيوانات المعرضة للإشعاع الكهرومغناطيسي والتي أكدتها التغيرات الكبيرة في معايير الشكل. بالإضافة إلى ذلك ، فيما يتعلق بإنزيمات مضادات الأكسدة ، كانت هناك زيادة في (malondialdehyde (MDA وانخفاض في ديسموتاز الفائق أكسيد (SOD) ، الجلوتاثيون (GSH) . انخفضت بشكل ملحوظ معاملات الحيوانات المنوية للفئران البالغة عند اليوم السابعين من الولادة في الحيوانات المعرضة مقارنة مع المجموعة الضابطة بالإضافة الى قلة فى عدد الحيوانات المنوية وحركتها وزيادة في الأشكال غير الطبيعية

الاستنتاج: قد تنجم آثار خطيرة عن التعرض المفرط للإشعاع الكهرومغناطيسي الناتج عن الهواتف المحمولة على نمو الخصية في الجرذان البيضاء.